⌘ *Author's Choice*

THE JOURNAL OF BIOLOGICAL CHEMISTRY VOL. 283, NO. 37, pp. 25576–25588, September 12, 2008

Thyroid Hormone Receptor α1 Follows a Cooperative CRM1/Calreticulin-mediated Nuclear Export Pathway*

Received for publication, December 24, 2007, and in revised form, June 9, 2008 Published, JBC Papers in Press, July 19, 2008, DOI 10.1074/jbc.M710482200

Matthew E. Grespin[1], Ghislain M. C. Bonamy[1,2], Vincent R. Roggero, Nicole G. Cameron, Lindsay E. Adam, Andrew P. Atchison, Victoria M. Fratto, and Lizabeth A. Allison[3]

From the Department of Biology, College of William and Mary, Williamsburg, Virginia 23187

The thyroid hormone receptor α1 (TRα) exhibits a dual role as an activator or repressor of its target genes in response to thyroid hormone (T_3). Previously, we have shown that TRα, formerly thought to reside solely in the nucleus bound to DNA, actually shuttles rapidly between the nucleus and cytoplasm. An important aspect of the shuttling activity of TRα is its ability to exit the nucleus through the nuclear pore complex. TRα export is not sensitive to treatment with the CRM1-specific inhibitor leptomycin B (LMB) in heterokaryon assays, suggesting a role for an export receptor other than CRM1. Here, we have used a combined approach of *in vivo* fluorescence recovery after photobleaching experiments, *in vitro* permeabilized cell nuclear export assays, and glutathione *S*-transferase pull-down assays to investigate the export pathway used by TRα. We show that, in addition to shuttling in heterokaryons, TRα shuttles rapidly in an unfused monokaryon system as well. Furthermore, our data show that TRα directly interacts with calreticulin, and point to the intriguing possibility that TRα follows a cooperative export pathway in which both calreticulin and CRM1 play a role in facilitating efficient translocation of TRα from the nucleus to cytoplasm.

The thyroid hormone receptor α1 (TRα)[4] is a member of the nuclear receptor superfamily of transcription factors. TRα acts as an intracellular receptor for thyroid hormone (T_3), thereby regulating expression of T_3-responsive genes associated with many aspects of development, growth, and metabolism. Among the nuclear receptors, TRα is particularly intriguing in that it can modulate transcription whether or not it is bound to T_3. Consistent with this dual role as an activator or repressor of transcription, at steady state TRα appears to be almost exclusively localized in the nucleus. However, we have shown that the receptor, in fact, shuttles rapidly between the nucleus and cytoplasm (1). Whereas the significance of this nucleocytoplasmic shuttling remains to be precisely characterized, this activity may be related directly to regulation of TRα target genes as well as to yet unknown non-genomic functions (2).

Nucleocytoplasmic shuttling occurs as a result of a dynamic balance between the recognition of nuclear localization signals (NLS) and nuclear export signals (NES) by particular import and export factors termed importins and exportins, respectively (3). Most nuclear receptors appear to enter the nucleus via importin α/β recognition and subsequent translocation through the nuclear pore complex (3, 4). Unlike nuclear import, however, the export pathways followed by nuclear receptors remain more elusive.

The most thoroughly studied and well characterized nuclear export pathway involves the exportin CRM1. Many shuttling transcription factors outside of the nuclear receptor superfamily follow a CRM1-dependent mechanism (5, 6). Like other nuclear receptors, however, TRα lacks the leucine-rich NES associated with classical CRM1-mediated nuclear export (1, 7). Concordantly, we have shown through interspecies heterokaryon assays that TRα nuclear export is not inhibited by leptomycin B (LMB), a potent inhibitor of CRM1 activity. These data clearly indicate that, at least in a heterokaryon system, TRα can use a CRM1-independent nuclear export pathway (1).

There is compelling evidence that suggests that the Ca^{2+}-binding protein calreticulin (CRT) may play a role in the nuclear export of several nuclear receptors (8–12). For example, the glucocorticoid receptor (GR) undergoes CRT-dependent nuclear export (11, 12) mediated through its highly conserved DNA binding domain (DBD) (8). However, the extent to which CRT functions as an export receptor has remained a subject of debate because its primary role is in the quality control of protein folding in the ER. In addition to this process, CRT has been implicated in an increasing number of critical cellular processes including regulation of Ca^{2+} homeostasis (13–15), integrin-mediated cell adhesion (16–18), numerous roles in immune response (19, 20), and cardiac muscle development (21–23).

As noted above, a widely used technique to study the subcellular trafficking of nuclear receptors has been the interspecies

* This work was supported, in whole or in part, by National Institutes of Health Grant 2R15 DK058028-02 and National Science Foundation Grant MCB-0646506 (to L. A. A.). This work was also supported by a Howard Hughes Medical Institute grant through the Undergraduate Biological Sciences Education Program to the College of William & Mary (to N. G. C., L. E. A., and A. P. A.). The costs of publication of this article were defrayed in part by the payment of page charges. This article must therefore be hereby marked "*advertisement*" in accordance with 18 U.S.C. Section 1734 solely to indicate this fact.

⌘ *Author's Choice*—Final version full access.

[1] Both authors contributed equally to this work.

[2] Current address: Dept. of Functional Genomics, Imaging Core, Genomic Institute of the Novartis Research Foundation, 10675 John Jay Hopkins Dr., San Diego, CA 92121.

[3] To whom correspondence should be addressed: P. O. Box 8795, Millington Hall 116, Williamsburg, VA 23187-8795. Tel.: 757-221-2232; Fax: 757-221-6483; E-mail: laalli@wm.edu.

[4] The abbreviations used are: TRα, thyroid hormone receptor α; TRβ, thyroid hormone receptor β; LMB, leptomycin B; FRAP, fluorescence recovery after photobleaching; CRT, calreticulin; NLS, nuclear localization signal; NES, nuclear export signal; GR, glucocorticoid receptor; DBD, DNA binding domain; ER, endoplasmic reticulum; PEG, polyethylene glycol; GST, glutathione *S*-transferase; GFP, green fluorescent protein; SV40, simian virus 40; DIC, differential interference contrast; RRL, rabbit reticulocyte lysate; RanBP3, Ran-binding protein 3; MEM, minimal essential medium; PBS, phosphate-buffered saline.

heterokaryon assay (1, 8, 24–28). Recently, it has been reported that the polyethylene glycol (PEG)-induced fusion of the cytoplasm during this assay disrupts the ER, thereby causing a transient elevation in cytosolic CRT levels as the protein is released from the ER lumen (29). This fusion process may alter the export kinetics of some shuttling proteins. For example, in contrast to the rapid shuttling of GR observed in heterokaryon assays (8, 25), GR shuttling was found to occur only slowly over a period of hours during fluorescence recovery after photobleaching (FRAP) experiments in monokaryons (29). Moreover, in contrast to heterokaryon fusion experiments in which GR shuttling was shown to be CRT-dependent (8), slow GR recovery in experiments other than heterokaryon fusions was shown to occur in a CRT-independent manner (29). Given these results, the question has arisen as to whether CRT-dependent nuclear export occurs under physiological conditions or merely in response to exogenous environmental stresses such as cell fusion.

With these data in mind we sought to ascertain whether TRα shuttles under physiological conditions and, if so, whether it follows a CRT or CRM1-dependent nuclear export pathway. To this end, we used a combined approach of *in vivo* FRAP experiments, *in vitro* digitonin-permeabilized cell nuclear export assays, and GST pull-down assays. Taken together, our *in vivo* and *in vitro* data point to the intriguing possibility that TRα uses an export pathway in which CRT binds directly to TRα and, thereby, promotes a cooperative interaction in which both CRT and CRM1 play a role in mediating rapid, efficient translocation of TRα from the nucleus to cytoplasm.

EXPERIMENTAL PROCEDURES

Plasmids—The plasmid pGFP-TRα encodes a functional GFP-TRα fusion protein expressed under human cytomegalovirus promoter control. This plasmid was constructed by subcloning the PCR product of rTRα1 (rat) cDNA into the enhanced GFP expression plasmid pEGFP-C1 (Clontech Laboratories, Inc.) using SacI and BamHI enzymes (1).

The plasmid pNES-GFP-GST-NLS was a gift from R. Haché (University of Ottowa, Ottowa, Ontario) and contains the classic HIV-1 Rev NES sequence cloned into the ApaI site of pGFP-GST-NLS, a plasmid that includes the sequence of the classic simian virus 40 (SV40) large T antigen NLS at the 3′ end (described further in Ref. 29). The plasmid pGEX-CRTwt was a gift from B. Paschal and encodes full-length calreticulin subcloned into the pGEX-KG vector for overexpression in bacteria (12). The plasmid pET-His-CRM1-H was a gift from J. Kjems and encodes His-CRM1 for overexpression in bacteria (28).

Cell Culture—HeLa cells (ATCC CCL-2) were cultured in MEM supplemented with 10% fetal bovine serum (Invitrogen) containing penicillin (100 units/ml)/streptomycin (100 μg/ml), at 37 °C under 5% CO_2 and 98% humidity. K41 ($crt^{-/-}$) and K42 ($crt^{+/+}$) cells were a generous gift from M. Michalak (30). These mouse embryonic fibroblasts were cultured in Dulbecco's modified Eagle's medium with 10% calf serum under similar conditions. Cells were grown to 70–90% confluency.

Transient Transfection and Live Cell Imaging—For transient transfections, cells were seeded at 4–7 $\times$ 10^5 cells per 60-mm vented dish (Nunc, Rochester, NY) onto 5-cm coverslips. Twenty-four h after seeding, cells at 40–60% confluency were transfected with 4 μg of plasmid DNA and 20 μl of Lipofectamine Reagent (Invitrogen) in Opti-MEM I Reduced Serum Medium (Invitrogen) according to the manufacturer's protocol. Reduced serum medium was replaced with complete medium 16–18 h post-transfection.

After transfection, cells were used for microscopy within 48 h. Prior to mounting in an enclosed perfusion chamber (Bioptechs, Butler, PA), coverslips were incubated in 2 ml of complete media containing 100 μg/ml cycloheximide (Sigma), penicillin (100 units/ml)/streptomycin (100 μg/ml), and 2–4 nM LMB (Sigma) or with vehicle (0.1% methanol) for 30 min. Coverslips were then washed with 2 ml of Dulbecco's phosphate-buffered saline (PBS) and mounted. For the duration of each experiment, cells were incubated in MEM or Dulbecco's modified Eagle's medium containing 50 μg/ml cycloheximide, penicillin (50 units/ml)/streptomycin (50 μg/ml), and 2–4 nM LMB or vehicle (0.1% methanol).

Images were collected from an inverted Nikon ECLIPSE TE 2000-E fluorescence microscope equipped with a Radiance 2100 laser scanning unit using a $\times$60 1.2 NA water objective (Nikon). The 488-nm line of a krypton-argon laser with a bandpass 515/30 nm emission filter was used for GFP detection and images were obtained using the time course module of Laser Sharp 2000 (Zeiss, Thornwood, NY).

FRAP was recorded to analyze shuttling of proteins between nuclei within monokaryons. All FRAP experiments were performed in a temperature-controlled setting using a FCS2 live-cell chamber heating system and objective heater system (Bioptechs) to maintain 37 °C. After the appropriate temperature was reached, an initial image was recorded from an area containing a multinucleated GFP-expressing cell using 2–8% laser power from the 488 nm line of a krypton-argon laser. One nucleus within the monokaryon was exposed at 50% laser power for two cycles using the same laser. After this bleaching exposure, sequential images were taken every 5 min for 11 cycles. To minimize undesired photobleaching, low laser intensities of 2–8% were again used for post-bleach images. For quantitative analysis of digitized images, fluorescence intensity values were generated using ImageJ (NIH). Bleached and unbleached nuclei were each considered as independent regions of interest. In addition, these values took into account the background brightness levels during each experiment. Intensity values were subsequently normalized so that the total fluorescence within each monokaryon after bleaching was equal to 1. Graphs were generated using Microsoft Excel.

Heterokaryon Assay—For the preparation of heterokaryons, $crt^{-/-}$ cells (K42) were seeded at 2–2.5 $\times$ 10^5 cells/well onto coverslips in 6-well dishes. Cells were then transfected with a GFP-TRα expression vector. Twenty-four hours post-transfection of the $crt^{-/-}$ cells, human HeLa cells were trypsinized and resuspended in heterokaryon growth medium containing 70% Dulbecco's modified Eagle's medium, 10% fetal bovine serum, and 20% sterile distilled water. The resuspended cells were then plated on the same coverslips at 5–6 $\times$ 10^5 cells/well. The cells were then incubated for 2.5 h in the presence of cycloheximide at 50 μg/ml followed by 30 min in media with cycloheximide at 100 μg/ml at 37 °C to allow adherence. Subsequently, the cells

were rinsed with Dulbecco's PBS. For cell fusion, coverslips were placed on 100-μl drops of warm 50% polyethylene glycol 1500 (Roche Applied Science, Indianapolis, IN) and incubated for exactly 2 min. Each coverslip was then rinsed with Dulbecco's PBS and incubated for 2 h at 37 °C in heterokaryon growth media containing 100 μg/ml cycloheximide.

Following incubation, the cells were rinsed with Dulbecco's PBS and then fixed for 10 min in 3.7% formaldehyde. After three 5-min washes with Dulbecco's PBS, the cells were permeabilized using 0.2% Triton X-100. Following three 5-min washes with Dulbecco's PBS the cells were incubated in 200 μl of 1.5% normal goat serum for 20 min. The cells were then washed with Dulbecco's PBS and incubated for an additional 20 min in 1.5% normal goat serum containing 0.5 units/ml rhodamine-phalloidin (Molecular Probes, Eugene, OR) to visualize actin. Following a wash in Dulbecco's PBS, the cells were then incubated for 10 min in Dulbecco's PBS containing 10 μg/ml Hoechst 33258 (Sigma) to visualize DNA. Finally, the coverslips were mounted on slides using GelMount mounting media (Biomeda, Foster City, CA). Slides were examined by fluorescence microscopy and images were obtained with a CoolSNAP HQ_2 CCD camera (Photometrics, Tucson, AZ) and NIS-Elements software (Nikon).

Antibody Staining—Cells were grown to 80–90% confluency and plated at 2×10^5 cells/well onto coverslips in six-well dishes (Nunc). 24 h post-plating, coverslips were incubated in 2 nM LMB or 0.1% methanol for 5 h. The cells were then fixed and permeabilized. After fixation and permeabilization, cells were incubated in 1.5% normal goat serum in Dulbecco's PBS for 30 min. The cells were then washed in Dulbecco's PBS and probed for 1 h in blocking solution containing rabbit polyclonal anti-CRT antibodies (Stressgen, Ann Arbor, MI) diluted to 1:1000. Cells were then washed in Dulbecco's PBS three times for 5 min each prior to incubation for 1 h with fluorescein isothiocyanate-conjugated goat anti-rabbit IgG (Vector Laboratories, Burlingame, CA) diluted to 1:600. After incubation the cells were washed in Dulbecco's PBS and mounted using GelMount containing 4′,6-diamidino-2′-phenylindole dihydrochloride (Sigma) (0.5 μg/ml). CRT staining was visualized by fluorescence microscopy.

Nuclear Extractions—Cells were plated at $1–2 \times 10^7$ and grown for 24 h to confluence in 100-mm vented dishes. Cells were rinsed 3 times in Dulbecco's PBS and nuclei lysed in 1 ml of Cell Lysis Solution (10 mM Hepes, pH 7.9, 10 mM KCl, 10 mM EDTA pH 8.0, 0.4% IGEPAL (Sigma), 0.5 mM phenylmethylsulfonyl fluoride (Roche), 1 mM dithiothreitol (dithiothreitol) (Omnipur, Gibbstown, NJ), Complete Mini EDTA-free Protease Inhibitor Mixture Tablet (1 tablet/10 ml) (Roche) for 10 min at 4 °C. The lysed cells were scraped and sheared by four passages through a 21-gauge needle. The quality and purity of the nuclei were monitored by differential interference contrast (DIC) microscopy at ×600; shearing was repeated until >95% of nuclei were visibly free from ER and other cytoplasmic contamination. Nuclei were pelleted by a 5-s pulse spin ($200 \times g$) at 4 °C in a microcentrifuge. The cytoplasmic fraction was collected and the purified nuclei were washed twice with 1 ml of extraction solution. A small fraction of the resuspended nuclei from the last wash was observed by DIC to confirm that the nuclei had remained intact and were free from ER and other cytoplasmic debris. The nuclear proteins were then extracted with 100 μl of Nuclear Extraction Solution (20 mM Hepes, pH 7.9, 0.4 M NaCl, 10 mM EDTA, pH 8.0, 10% glycerol, 0.5 mM phenylmethylsulfonyl fluoride, 1 mM dithiothreitol, Complete Mini EDTA-free Protease Inhibitor Mixture Tablets (1 tablet/10 ml)). Proteins from nuclear and cytoplasmic fractions were then analyzed by Western blot.

Western Blotting—The approximate concentration of total protein in nuclear and cytoplasmic samples was determined by absorption at 280 nm. For cytoplasmic and whole cell extract, 40 μg of protein were analyzed per lane, 40–60 μg per lane were used for nuclear extracts, and 0.5–2 μl of rabbit reticulocyte lysate (RRL) (Promega, Madison, WI) were analyzed. The samples were separated by 8% SDS-PAGE and transferred to polyvinylidene difluoride membranes (Amersham Biosciences) by semi-dry electroblotting (Bio-Rad). The membranes were incubated overnight in the presence of blocking solution (Tris-buffered saline (TBS), 1% bovine serum albumin, 0.1% Tween 20). After six washes with TBS, the membranes were incubated with the primary antibodies for 1 h. For the detection of CRT and β-tubulin both rabbit polyclonal anti-CRT antibodies (SPA-600D, Stressgen) and rabbit polyclonal anti-β-tubulin antibodies (Affinity Bioreagents, Golden, CO) were mixed together in blocking solution at 1:20,000 and 1:200, respectively. For the detection of CRM1 and CRT, Western blots were incubated separately with anti-CRM1 (Affinity Bioreagents) or anti-CRT (Stressgen) antibodies at 1:200 or 1:20,000, respectively. The blots were then washed six times with TBS and incubated with a horseradish peroxidase-conjugated goat anti-rabbit IgG (GE Healthcare) at 1:30,000 for 1 h in blocking solution. Following this incubation, the blots were washed again six times and incubated with ECL-Plus detection reagent (GE Healthcare). Subsequently, the blots were analyzed using a Storm 860 Molecular Imager scanner (GE Healthcare) and ImageJ (NIH).

Protein Overexpression—Plasmids coding for the protein of interest were transformed into competent *Escherichia coli* (BL21 DE3-RIl) (Stratagene, La Jolla, CA), per the manufacturer's protocol, and grown to an A_{600} of 0.6–0.8 at 37 °C. Expression was induced with 0.5 mM isopropyl β-D-thiogalactoside (Fisher Scientific, Pittsburgh, PA) and grown 3–5 h at 30 °C. Post-expression cultures were centrifuged at $1,700 \times g$ for 15 min at 4 °C; bacterial pellets were stored at −80 °C prior to protein purification.

GST Protein Purification—Bacterial pellets were resuspended in 10 ml of B-PER® Bacterial Protein Extraction Reagent (Pierce), 1 ml of 5.0 mg/ml lysozyme (Fisher), 10 mM Tris, pH 8.0, and one Complete Mini EDTA-free Protease Inhibitor Mixture tablet (Roche). Resuspended pellets were incubated on ice for 30 min. The pellets were subsequently sonicated (Sonic Dismembrator model 100; Fisher) on ice to fully lyse the bacteria. The lysed mixture was then centrifuged at $17,950 \times g$ for 15 min at 4 °C, and the supernatant was applied to 200 μl of 50% glutathione-Sepharose 4B resin (GE Healthcare). Samples were incubated for 60 min at 4 °C with gentle rotation, then centrifuged for 5 min at $500 \times g$ at 4 °C to pellet the resin. The resin pellet was washed 3 times with 10 ml of ice-cold PBS (140 mM

NaCl, 2.7 mM KCl, 10 mM Na_2HPO_4, 1.8 mM KH_2PO_4, pH 7.3) and then transferred to a Microfilter Spin Column (Pierce) and washed twice with 600 μl of ice-cold PBS. 100 μl of Glutathione Elution Buffer (10 mM glutathione) was added to the column, incubated at room temperature for 2–4 min with agitation, then centrifuged at 700 × *g* for 30 s at 4 °C to collect eluted protein. The elution step was repeated 3 times. The eluted fractions were pooled and dialyzed (Slide-A-Lyser® Mini Dialysis Units, 7000 MWCO, Pierce) against Dulbecco's PBS overnight at 4 °C. Protein samples were then concentrated using Micron Ultracel YM-30 Centrifugal Filter Devices (Millipore, Bedford, MA). Concentrated protein samples were analyzed by SDS-PAGE and protein concentration estimated using a NanoDrop® ND-1000 full-spectrum UV-Visual Spectrophotometer. Samples were stored at −80 °C.

Permeabilized Cell Nuclear Export Assays—HeLa cells were seeded on 22-mm Coverslips for Cell Growth™ (Fisher) in 6-well culture dishes (Nunc) at a concentration of 2–3 × 10^5 cells per well. 24 h post-seeding each well was transiently transfected with 2 μg of plasmid DNA and 10 μl of Lipofectamine reagent (Invitrogen) in Opti-MEM I reduced serum medium, and incubated 12–16 h. After 12–16 h Opti-MEM I was replaced with MEM containing 10% fetal bovine serum. After 4 h cells were washed 3 times with 2 ml/well of ice-cold export buffer (20 mM Hepes, pH 7.3, 110 mM KOAc, 5 mM NaOAc, 2 mM $Mg(OAc)_2$, 1 mM EGTA, 2 mM dithiothreitol, 1 mM phenylmethylsulfonyl fluoride, Complete Mini EDTA-free Protease Inhibitor Mixture tablet (1 tablet/10 ml) (Roche), then permeabilized with digitonin (50 μg/ml; Calbiochem, San Diego, CA) in export buffer for 4.5 min. Subsequently, cells were rinsed with 2 ml/well of ice-cold export buffer for 10 min. Coverslips were then inverted over 50-μl drops of export reaction mixture (energy regeneration system composed of 5 mM creatine phosphate, 20 units/ml creatine phosphokinase, 0.5 mM ATP, 0.5 mM GTP, 5× export buffer, 670 nM GST-CRT, and 25 μl of RRL) on parafilm in a moist chamber for 30 min at 30 °C. Cells were then fixed in 3.7% formaldehyde (Fisher) for 10 min followed by a 5-min rinse with export buffer. Coverslips were subsequently mounted on slides with 8 μl of GelMount with 4′,6-diamidino-2′-phenylindole (0.5 μg/ml), and viewed by fluorescence microscopy.

GST Pull-down Assays—Pull-down assays using GST-CRT were performed using the ProFound Pull-down GST Protein: Protein Interaction Kit (Pierce), and modified amounts of GST resin/protein. GST resin was equilibrated with five 0.5-ml washes of TBS (25 mM Tris·HCl, 0.15 M NaCl, pH 7.2):ProFound Lysis Buffer (1:1). Bait protein immobilization was performed at 4 °C for 30 min with gentle rocking. For GST-CRT/His-CRM1 interactions, 50 μl of 50% GST resin was used to bind 40 μg of GST-CRT bait protein. For GST-CRT/His-TRα and GST-CRT/His-TRα/His-CRM1 interactions, 5 μl of 50% GST resin was used to bind 4 and 7 μg of GST-CRT bait protein, respectively. Bound bait protein was washed 5 times with 0.5 ml of TBS:ProFound Lysis Buffer (1:1). Prey protein capture was performed at 4 °C for 1 h with gentle rocking. For GST-CRT:CRM1, GST-CRT:TRα binding, and GST-CRT:TRα:CRM1, 40 μg of His-CRM1, 2 μg of His-TRα (Active Motif, Carlsbad CA), and 3.5 μg of His-TRα, 3.5 μg of His-CRM1 prey were used. Bait-Prey elution was performed with 50 μl of 100 mM Glutathione Elution Buffer for GST-CRT/CRM1 interactions, and 12.5 μl for GST-CRT/TRα and GST-CRT/TRα/CRM1 interactions. All elutions were analyzed via SDS-PAGE using an 8–16% precast Gene Mate Express Gel (ISC BioExpress, Kaysville, UT). Gels were stained with SimplyBlue™ SafeStain (Invitrogen) and imaged using a Bio-Rad Gel Doc XR documentation system with Quantity One analysis software (version 4.6.1).

Coimmunoprecipitation Assays—For coimmunoprecipitation assays, HeLa, $crt^{-/-}$, and $crt^{+/+}$ cells were transfected with expression vectors for GFP-TRα, or GFP alone as a control, in 100-mm plates using Lipofectamine 2000 (Invitrogen). 20 h post-transfection, the medium was replaced with medium containing 2–4 nM LMB or vehicle (0.1% methanol). Cells were lysed 5 h later and nuclear extracts were prepared using a Nuclear Extract Kit (Active Motif) according to the manufacturer's instructions. Nuclear extracts were incubated with anti-CRT antibodies bound to Dynal Dynabeads® Protein G (Invitrogen) for 2 h at 4 °C. The immunoprecipitated material was captured on a DynaMag™-2 magnetic particle concentrator, washed, and eluted in SDS-PAGE sample buffer. Samples of immunosupernatants and immunoprecipitated material were separated by 8% SDS-PAGE. Replicate Western blots were prepared and probed with anti-CRT, anti-CRM1, and anti-GFP (Santa Cruz Biotechnology Inc.) antibodies, followed by chemiluminescent detection.

RESULTS

TRα Shuttling in Living Cells Is Leptomycin B Sensitive—The thyroid hormone receptor is a dynamic protein that shuttles rapidly between the nucleus and cytoplasm in heterokaryon assays. This shuttling is not blocked by LMB in heterokaryons, indicating that TRα is exiting the nucleus by a CRM1-independent pathway in the heterokaryon assay (1). The heterokaryon assay involves PEG-induced fusion of the cytosols of transfected cells of one species (*e.g.* mouse) with untransfected cells of another species (*e.g.* human). Movement of the protein of interest can then be monitored from the nuclei of transfected cells into the shared cytosol of the fused cells and, subsequently, into the nuclei of the opposing species. The recent finding that PEG-induced cell fusion causes changes in the cellular environment including a transient elevation in CRT levels (29) has called into question the validity and interpretation of previous heterokaryon experiments.

We first sought to determine whether TRα shuttles under physiological conditions by performing experiments in living cells, independent of heterokaryon formation. To maintain physiological conditions, we used a FRAP assay in multinucleate live cells (monokaryons) to monitor the movement of GFP-TRα from unbleached to bleached nuclei. Unlike in heterokaryons, a monokaryon system does not require cell fusion or other manipulation that would compromise the integrity of the ER and thus, presumably, maintains low levels of cytosolic CRT. Transfected monokaryons were selected and one nucleus within these cells was exposed to intense laser illumination. This exposure resulted in loss of fluorescence within the selected nucleus due to irreversible photobleaching of the GFP

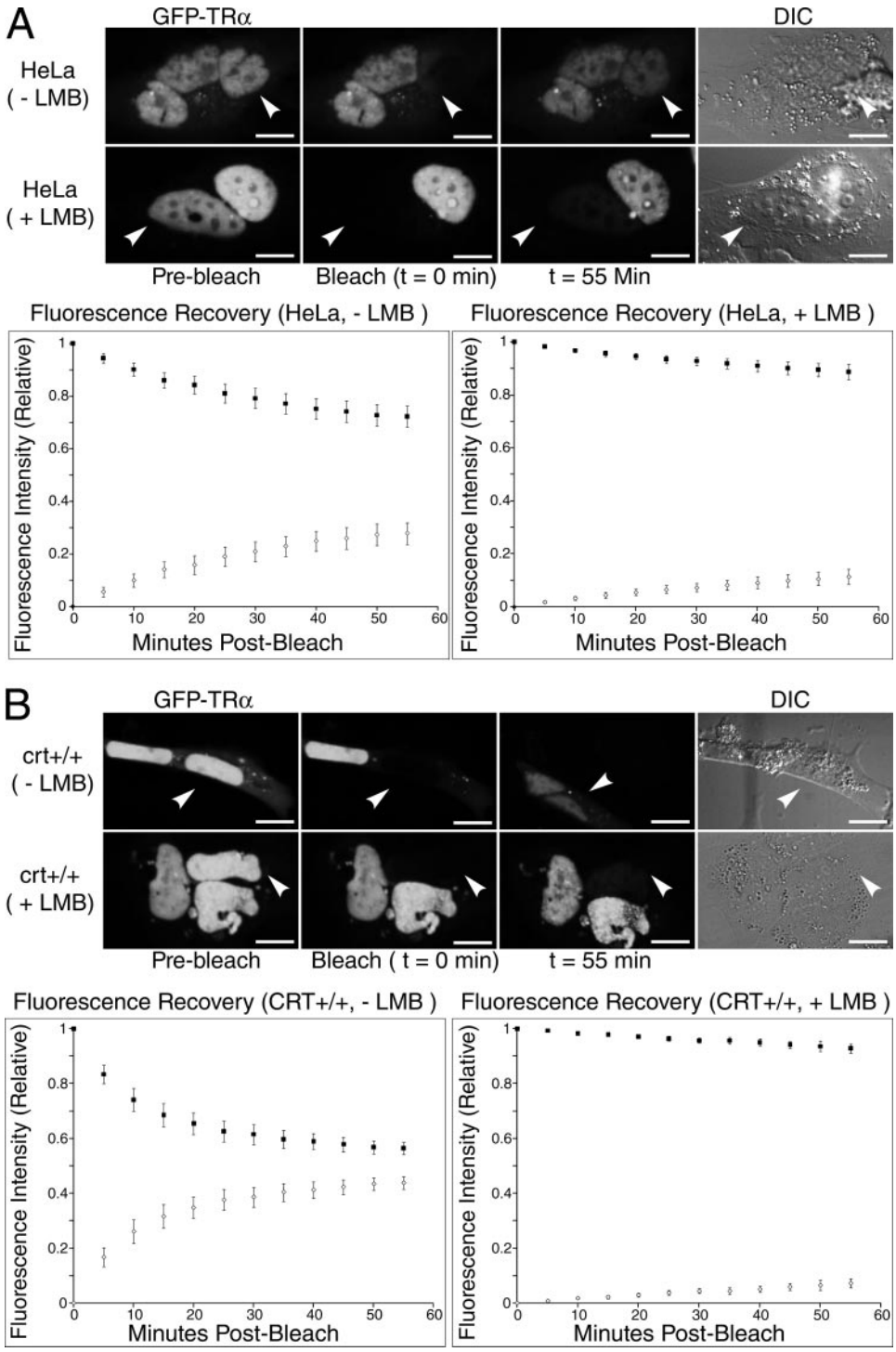

FIGURE 1. **TRα shuttling is inhibited by treatment with LMB in live monokaryons expressing CRT.** *A*, HeLa cells were transfected with a GFP-TRα expression plasmid and nucleocytoplasmic shuttling was monitored through FRAP ($n = 7$). *White arrowheads* indicate photobleached nuclei. Parallel experiments were performed in the presence of LMB ($n = 6$) to block CRM1-mediated nuclear export and DIC images were taken to delineate cell borders. Fluorescence recovery graphs indicating relative shuttling of GFP-TRα were generated. *Black squares* indicate relative fluorescence levels within unbleached nuclei and *open diamonds* represent levels within bleached nuclei. Any apparent change in nucleus morphology is a result of cell movement over the course of the experiment. *Error bars*, ± 1 S.E. *B*, as in *A* using $crt^{+/+}$ cell line ($n = 10$, −LMB; $n = 6$, +LMB). *Bar*, 10 μm.

fluorophore. The initial bleaching did not, however, result in loss of fluorescence to neighboring nuclei within the same cells (Fig. 1). A series of images was taken for each individual experiment in which fluorescence recovery to bleached nuclei was measured and compared with the concomitant decrease in intensity within unbleached nuclei. Through image analysis and plotting of these fluorescence intensity data, we were able to determine the relative degree of nucleocytoplasmic shuttling within particular cell types and treatments. Specifically, we assayed for TRα shuttling in human HeLa and mouse $crt^{+/+}$ cell lines, both of which express CRT. We show that, in contrast to the slow nuclear export observed for GR in COS-7 cells (29), TRα in fact shuttles rapidly between nuclei in both HeLa (Fig. 1*A*) and $crt^{+/+}$ monokaryons (Fig. 1*B*). These data are in close agreement with those observed for TRα shuttling kinetics in heterokaryons (1), and suggest that TRα may play an as yet unknown role in cytosolic signaling pathways. After confirming that TRα rapidly shuttles between nuclei in these cells, we sought to determine whether TRα follows a CRM1 or CRT-dependent nuclear export pathway in live, unfused cells.

Based on our previous data showing that TRα nucleocytoplasmic shuttling is not blocked by LMB in a heterokaryon system (1), we predicted that we would observe rapid shuttling of TRα between nuclei when HeLa and $crt^{+/+}$ monokaryons were treated with LMB. Surprisingly, we saw only slow recovery of TRα within photobleached monokaryon nuclei of both cell types during FRAP experiments (Fig. 1). In contrast to previous data for heterokaryons in which near complete equilibration between nuclei was seen over the course of 1 h (1), recovery of fluorescence to bleached nuclei within live monokaryons treated with LMB was limited to only 22% (±3%) for HeLa cells and 14% (±2%) for $crt^{+/+}$ cells over a similar time course (Fig. 1). These results are in sharp contrast to parallel FRAP experiments performed in the absence of LMB, during which TRα shuttling was much more rapid. In these experiments recovery to the bleached nuclei was measured at 56% (±4%) equilibration for HeLa cells and 88% (±2%) equilibration for $crt^{+/+}$ cells over 1 h (Fig. 1). To graphically illustrate the

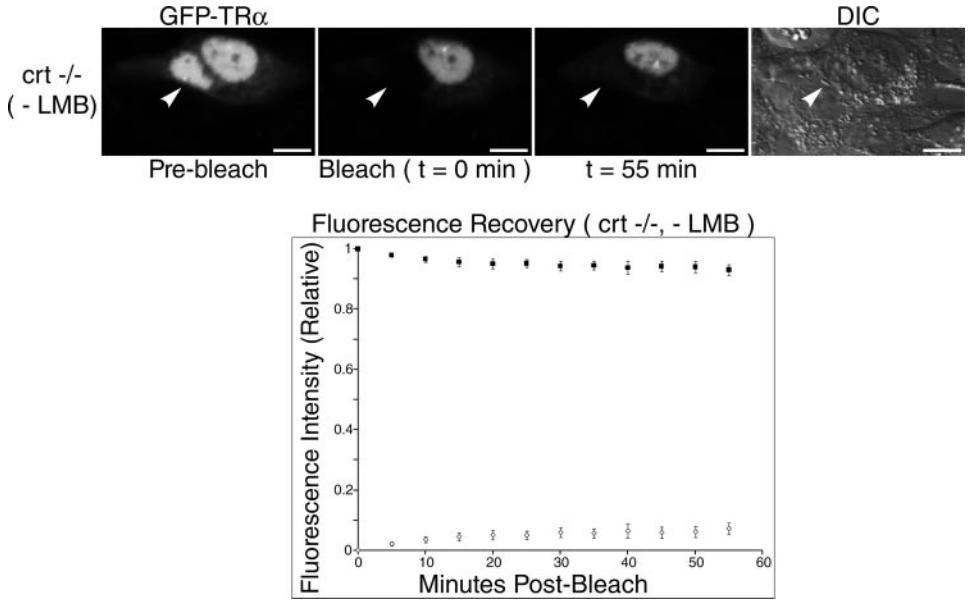

FIGURE 2. **TRα requires CRT for nuclear export.** $crt^{-/-}$ cells were transfected with a GFP-TRα expression plasmid and nucleocytoplasmic shuttling was monitored through FRAP ($n = 8$). *White arrowheads* indicate bleached nuclei. DIC images were taken to delineate cell borders and a fluorescence recovery graph indicating relative shuttling of GFP-TRα was generated. *Bar*, 10 μm.

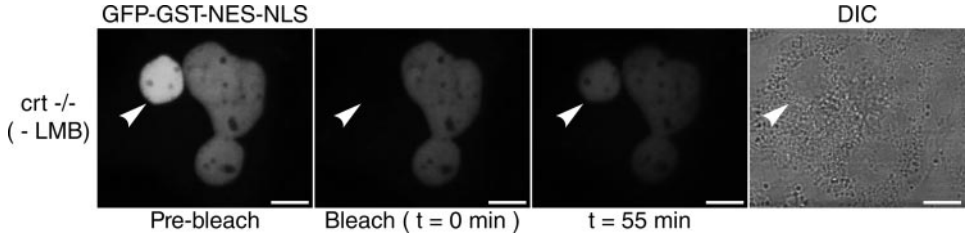

FIGURE 3. **The CRM1-mediated nuclear export pathway is active in $crt^{-/-}$ cells.** An expression plasmid for a CRM1-dependent shuttling control protein (GFP-GST-NES-NLS) was transfected into $crt^{-/-}$ cells and nucleocytoplasmic shuttling was monitored by FRAP. *White arrowheads* represent bleached nuclei. *Bar*, 10 μm.

sensitivity of TRα nucleocytoplasmic shuttling to LMB, mean brightness values for photobleached and unbleached nuclei were plotted as a function of time post-bleach. Fluorescence intensity was normalized so that the overall fluorescence of bleached and unbleached nuclei was equal to 1.0 (arbitrary units). After normalization, convergence of the representative curves for bleached nuclei and unbleached nuclei toward one another represents the degree of fluorescence equilibration between these compartments. When one bleached and one unbleached nucleus are present, complete equilibration occurs at 0.5 fluorescence units.

To ensure that any recovery in GFP signal to bleached nuclei occurred as a result of nucleocytoplasmic shuttling and not as a result of *de novo* protein synthesis, all experiments were performed in the presence of cycloheximide. DIC microscopy was also performed to visualize monokaryon borders, thereby confirming that the experiments in which no shuttling was observed were conducted in cells that were, indeed, multinucleated as opposed to adjacent independent cells.

Taken together, these data show that TRα nuclear export is LMB-sensitive, suggesting that in live, unfused cells the CRM1 pathway plays a role in mediating export of TRα. One possible explanation for these unexpected results is that the heterokaryon system used previously to assay for CRM1 dependence (1) creates an artificial environment in which the effects of deactivating CRM1 activity are overshadowed by cell fusion-dependent up-regulation of alternative export factors such as CRT. With this possibility in mind, we sought to determine whether CRT is used as an alternative, or cooperative, nuclear export receptor by TRα *in vivo*.

TRα Shuttling Is Inhibited in Living Cells Deficient in CRT Expression—CRT has previously been shown to function as an exportin for nuclear receptors related to TRα (8, 11, 12, 31). To address the question of whether TRα export is also mediated by CRT, we transiently transfected mouse embryonic fibroblast cells isolated from CRT knock-out mouse embryos ($crt^{-/-}$ cells) (23) with GFP-TRα and monitored FRAP in bleached nuclei of transfected CRT-deficient monokaryons (Fig. 2).

Prior to analysis of nuclear export, we first assessed the ability of TRα to enter the nucleus of $crt^{-/-}$ cells. Although nuclear import of both the tumor suppressor p53 and the transcription factor NF-AT3 are impaired in cells deficient in CRT expression, other shuttling proteins including GR and GATA4 are unchanged in their import properties regardless of whether CRT is present (32). Thus, the altered nuclear import of some proteins in $crt^{-/-}$ cells is a specific effect and is not indicative of a general defect in the import cycle. Nuclear import of TRα was not impaired in $crt^{-/-}$ cells, indicating that CRT is not required for its nuclear localization (Fig. 2).

Although TRα remained localized to $crt^{-/-}$ cell nuclei prior to FRAP, we observed a striking reduction in its nucleocytoplasmic shuttling after photobleaching (Fig. 2). Indeed, only 14% (±2%) fluorescence equilibration from unbleached nuclei to bleached nuclei was seen in the $crt^{-/-}$ cell line. In contrast, HeLa cells and $crt^{+/+}$ cells not treated with LMB showed 56% (±4%) and 88% (±2%) fluorescence equilibration with unbleached nuclei, respectively (Fig. 1). To demonstrate that the lack of CRT in these cells was not responsible for any nonspecific action preventing all nucleocytoplasmic shuttling, $crt^{-/-}$ cells were also transfected with a shuttling control construct, pNES-GFP-GST-NLS. The fusion protein localizes to the nucleus at steady state and shuttles via a CRM1-mediated nuclear export pathway (29). As expected, shuttling of this protein was not inhibited in $crt^{-/-}$ cells, indicating that the CRM1 pathway is functional in these cells ($t_{1/2} < 10$ min) (Fig. 3). Taken together, these data support the hypothesis that TRα can follow a CRT-mediated nuclear export pathway.

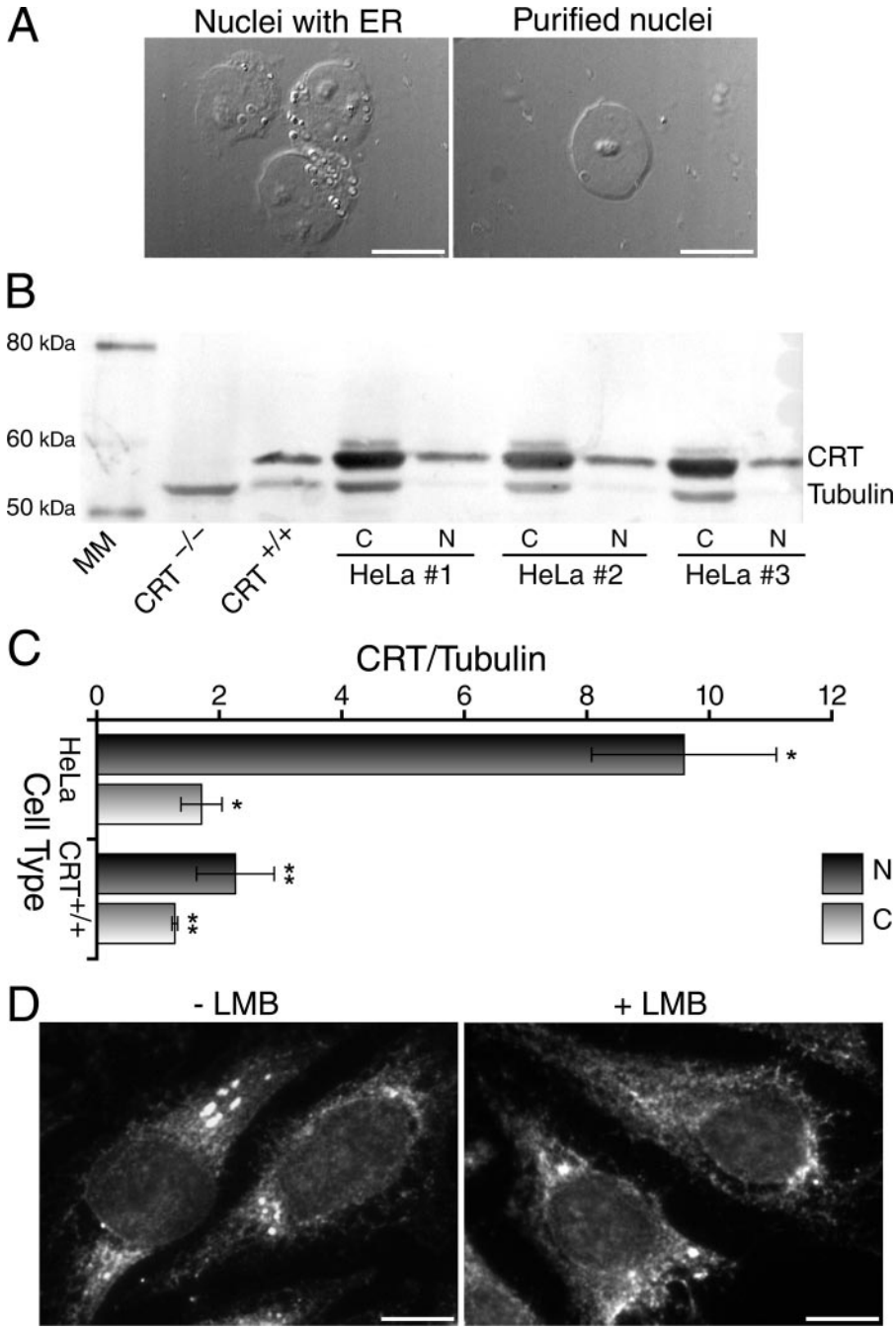

FIGURE 4. **CRT is localized to the cytosol and nuclei of various cell types.** *A*, to ensure that purified nuclei were free of ER and other cytoplasmic contaminants, nuclear fractions were monitored by DIC. *Left panel*, a clump of nuclei with residual ER and cytoplasmic debris; these nuclei were subjected to additional purification steps prior to use (see "Experimental Procedures"). *Right panel*, an isolated nucleus free of residual ER and other cytoplasmic contaminants. *B,* proteins extracted from purified nuclei and cytosolic fractions from HeLa and $crt^{+/+}$ cells were analyzed by Western blot, using anti-CRT and anti-β tubulin antibodies. Magic Marker (*MM*) size standard is indicated and $crt^{-/-}$ cells were used as a negative control. A representative blot for HeLa cells is shown. *C,* the ratio of CRT to tubulin increased significantly from cytosolic to nuclear fractions in both HeLa cells ($n = 12$, *, $p < 0.001$) and $crt^{+/+}$ cells ($n = 13$, **, $p < 0.001$). *Error bars*, 99.9% confidence interval. *D,* HeLa cells incubated for 5 h in the presence or absence of LMB, as indicated, were fixed and labeled with anti-CRT antibodies by indirect immunofluorescence. *Bar*, 10 μm.

CRT Is Localized to the Cytoplasm and Nuclei of Various Cell Types—Previously, CRT was believed to reside solely in the ER. Recently, however, increasing numbers of reports have identified small fractions of CRT in both the cytosolic and nuclear compartments of various cell lines in addition to its primary location within the ER (33–35). To assess whether a detectable population of CRT was localized to the nuclei of the cells used in our study, we isolated nuclei by biochemical fractionation. To ensure that the nuclei extracted were free of ER and other cytoplasmic contamination, during the purification process nuclei were monitored by DIC at high resolution (Fig. 4*A*). Purification steps were repeated until only nuclei that were free of ER and other cytoplasmic debris remained. Proteins were extracted from the cytoplasmic fraction and from the purified nuclei and analyzed by Western blot. Blots were probed simultaneously with anti-CRT and anti-β tubulin, which was used to normalize the data. When comparing the amount of CRT in purified nuclei to the amount of tubulin, a strictly cytoplasmic protein, we found that the purified nuclei from HeLa cells were significantly enriched in CRT ($p < 0.001$) (Fig. 4, *B* and *C*). In HeLa cells, the ratio between CRT and tubulin increased from 1.7 $\pm$ 0.3 in the cytoplasm to 9.6 $\pm$ 4.2 in the nucleus indicating that the amount of CRT observed in the purified nuclei is not a result of residual cytoplasmic contamination. These results were also significant in $crt^{+/+}$ cells ($p < 0.001$) (Fig. 4, *B* and *C*). In these cells, the ratio between CRT and tubulin increased from 1.3 $\pm$ 0.1 in the cytoplasm to 2.3 $\pm$ 0.7 in the purified nuclei. Together these data provide further evidence that CRT is present in a small but significant fraction within the nucleus in the cell lines used for our experiments. To further demonstrate that CRT is localized to multiple cellular compartments, we performed indirect immunofluorescence assays. Consistent with the Western blot analysis a small population of nuclear CRT was observed in addition to a more prominent cytoplasmic pool (Fig. 4*D*).

TRα nuclear export is partially inhibited by treatment with LMB (Fig. 1). This suggests a role for CRM1 in TRα shuttling, in addition to that played by CRT, and points to a possible interplay between CRT and CRM1. A direct interaction between CRT and CRM1 could, in theory, induce a shift in CRT toward the nucleus upon treatment with LMB, which would be indic-

ative of CRM1 sequestering CRT in this compartment. To test this, we treated cells with LMB and performed immunostaining for CRT *in situ*. This treatment did not, however, induce a detectable shift in the subcellular localization of CRT toward the nucleus (Fig. 4*D*); a comparable population of nuclear CRT was observed in both LMB-treated and untreated cells.

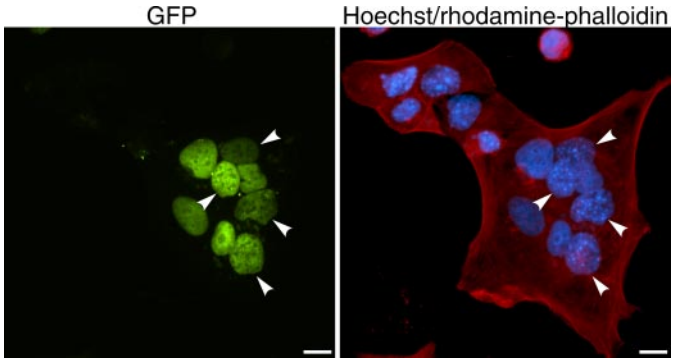

FIGURE 5. **Addition of CRT to CRT-deficient cells restores rapid nucleocytoplasmic shuttling and promotes export of thyroid hormone receptor (TRα) from CRT-deficient cell nuclei.** $crt^{-/-}$ cells were transfected with a GFP-TRα expression plasmid. Subsequently, CRT-expressing HeLa cells were plated on the same coverslip and cytoplasmic fusion was performed using 50% PEG. *Left panel*, cells were fixed and GFP-TRα localization was observed by fluorescence microscopy. Nuclei of $crt^{-/-}$ cells are indicated by *white arrowheads*. *Right panel*, HeLa cell nuclei exhibit diffuse Hoechst staining, whereas $crt^{-/-}$ have a speckled appearance. Heterokaryon borders are visualized by staining of F-actin with rhodamine-phalloidin. *Bar*, 10 μm.

Polyethylene Glycol-induced Heterokaryon Formation Restores TRα Export from CRT-deficient Cell Nuclei—Having shown that TRα nuclear export is impaired in $crt^{-/-}$ cells (Fig. 2), we sought to test whether TRα export could be restored by the addition of exogenous CRT. To do so, we transfected $crt^{-/-}$ cells with GFP-TRα and then fused them with untransfected HeLa cells. Because PEG-induced heterokaryon formation causes a transient elevation in cellular CRT levels (29), we hypothesized that if TRα uses CRT for nuclear export that the fusion process with CRT-expressing HeLa cells would restore export in $crt^{-/-}$ cells. This could occur either as a result of CRT release from the HeLa cell ER or, alternatively, from the relatively low CRT levels present within HeLa cell nuclei and cytosol prior to fusion. Experiments were performed in the presence of cycloheximide to inhibit *de novo* protein synthesis. Consistent with our prediction, we found that TRα was capable of exporting from $crt^{-/-}$ nuclei into the shared cytosol and subsequently reimporting into HeLa nuclei in these heterokaryon assays (Fig. 5). Taken together, the results from these heterokaryon experiments and our live-cell FRAP experiments support the hypothesis that TRα uses CRT as a nuclear export receptor.

Efficient Nuclear Export of TRα in Permeabilized Cells Requires Cytosol and CRT—To provide further evidence for a role of CRT in the nuclear export of TRα, we performed permeabilized cell *in vitro* nuclear export assays utilizing purified recombinant GST-CRT. For this assay, HeLa cells were transiently transfected with a GFP-TRα expression plasmid. GFP-TRα displays a complete and strong nuclear fluorescence 16 h post-transfection. At this point the outer cell membrane was permeabilized with digitonin and export reactions were performed. First, we sought to assess whether exogenous CRT was sufficient to induce nuclear export of TRα. Our results showed no observable change in TRα nuclear localization between 0 and 40 min irrespective of varying CRT concentration from 270 nM to 1 μM. During this period, all TRα remained localized to the nucleus (Fig. 6*A*).

To determine whether additional factors were required to either permit nuclear import of CRT or to aid in the nuclear export of TRα in conjunction with CRT, export reactions containing CRT and a cytosol mixture (RRL) alone or a combination of CRT and RRL were similarly assayed at 0 and 40 min. RRL is commonly used as a source of cytosol for nuclear import and export assays (36). Initially, we tested RRL alone. As expected, at t_0 TRα was localized

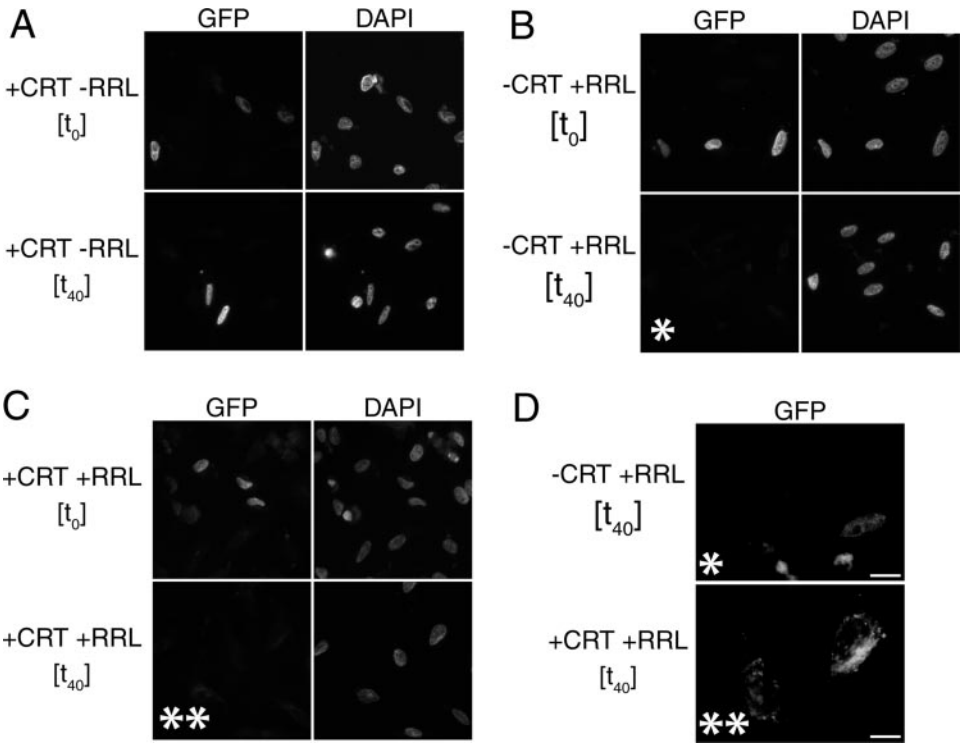

FIGURE 6. **Nuclear export of thyroid hormone receptor (TRα) in permeabilized cells.** *A*, GFP-TRα remains nuclear at t_{40} in the presence of 670 nM CRT. HeLa cells transfected with a GFP-TRα expression plasmid were digitonin permeabilized, and incubated in an export reaction containing CRT, energy regeneration system, and export buffer alone. At t_{40} no GFP-TRα export was observed. *B*, export reactions containing RRL, energy regeneration system, and export buffer were able to support >80% loss of nuclear fluorescence of GFP-TRα at t_{40}. *C*, export reactions containing both CRT and RRL were able to support >95% loss of nuclear fluorescence of GFP-TRα at t_{40}. *White* values were normalized to 2,000 using IPlab 3.55 for *A–C*. *D*, enlarged section from *panels B*, t_{40} (*), and *C*, t_{40} (**). *White* values for * from *panel B* and ** from *panel C* were adjusted to 200 for low intensity visualization of the residual GFP-TRα in export reactions. *Bar*, 10 μm.

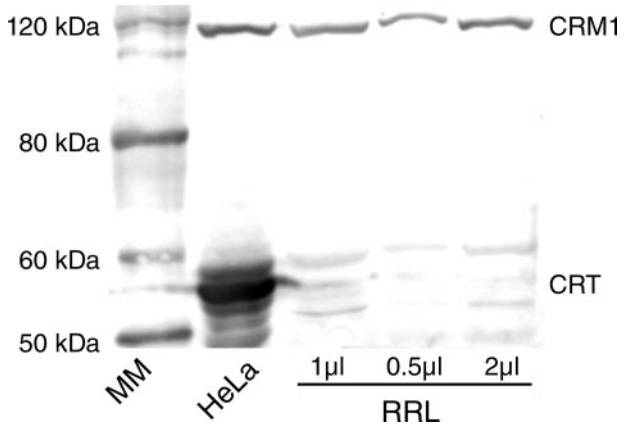

FIGURE 7. **RRL contains CRM1 but not CRT.** HeLa whole cell extract and varying volumes of RRL were subject to Western blot analysis, using anti-CRM1 and anti-CRT antibodies. Magic Marker (*MM*) size standard is indicated.

to the nucleus. At t_{40} a moderate level of export was observed as indicated by a decrease in GFP-TRα fluorescence in the nuclei compared with t_0 (>80% loss of fluorescence) (Fig. 6, *B* and *D*). Upon addition of RRL and CRT in combination, however, we observed a striking increase in the nuclear export of TRα as compared with that which was observed for RRL or CRT individually. Indeed, over a similar time course nuclear export was nearly complete (>95% fluorescence loss) (Fig. 6, *C* and *D*). These data suggest that an additional factor (or factors) present in the cytosol interacts cooperatively with CRT to mediate efficient nuclear export of TRα.

The GTPase Ran plays an integral role in the shuttling of many transcription factors and exists predominantly in a GTP-bound state within the nucleus. In this conformation, RanGTP participates in the formation of export complexes containing the classical leucine-rich NES (3, 4, 37, 38). In addition, it also stabilizes protein kinase inhibitor/CRT interactions as well as enhances CRT-dependent nuclear export of protein kinase inhibitor in permeabilized cells (12). It has been shown in permeabilized cell nuclear export assays that residual nuclear RanGTP remaining in cells after permeabilization was sufficient to permit CRT-dependent nuclear export (12). To determine the role of Ran in the nuclear export of TRα, we performed assays with recombinant CRT in the absence of RanGTP or having supplemented the system with 1.9 μM RanGTP. We did not, however, observe any difference in TRα nuclear localization between these conditions; TRα remained localized to the nucleus in either case (data not shown). This suggests that RanGTP is not the limiting factor for TRα nuclear export.

Several factors may play a role in stabilizing CRT/cargo interactions, inducing a conformational shift in CRT, or in other nonspecific functions. Calcium, for example, modulates CRT conformation within the lumen of the ER (39) and also regulates CRT function as a chaperone for the T-cell protein perforin (40). In addition, Ca^{2+} enhances CRT-mediated nuclear export of GR-GFP but, interestingly, excess Ca^{2+} also inhibits classical NES-regulated nuclear export of Rev-GFP *in vitro* (15). We supplemented permeabilized cell export assays with 20 mM Ca^{2+} in the presence of CRT but observed no difference in TRα nuclear localization. Under these conditions TRα remained localized to the nucleus (data not shown). These results suggest that Ca^{2+} also is not the limiting factor required for nuclear export in these assays.

Based on our findings in live cells that the nuclear export of TRα shows partial CRM1 dependence (Fig. 1), we performed Western blot analysis to test whether CRM1 was present in RRL and could be the additional factor required for efficient CRT-dependent nuclear export. Our data show that CRM1 was present in RRL and HeLa cell extracts, whereas CRT was detected only in HeLa cell extract and was absent from RRL (Fig. 7). These findings point to the possibility that CRM1 could be the additional factor accounting for the enhanced export of TRα in *in vitro* export assays supplemented with RRL. A cooperative interaction between CRT and CRM1, whether direct or indirect, also accounts for the observation that TRα is not exported as efficiently from nuclei treated with RRL, as CRT is absent from this exogenous cytosol replacement.

TRα Interacts Directly with CRT—To determine whether interactions between TRα, CRT, and CRM1 during nuclear export are direct or indirect, GST pull-down assays were performed (Fig. 8). A GST-CRT fusion protein was incubated with His-tagged TRα (Fig. 8*A*), His-tagged CRM1 (Fig. 8*B*), or both (Fig. 8*C*), and the input (flow-through) and binding (elution) fractions were analyzed by SDS-PAGE. TRα interacted with GST-CRT (Fig. 8*A*, *lane 3*), but not with GST alone (Fig. 8*A*, *lane 5*). In contrast, all input CRM1 was present in the flow-through fraction (Fig. 8*B*, *lane 5*); no CRM1 bound specifically to CRT alone (Fig. 8*B*, *lane 6*), or together with TRα (Fig. 8*C*, *lane 4*). Supplementing *in vitro* binding assays with RRL had no effect on complex formation (data not shown). Complex formation in HeLa, $crt^{+/+}$, and $crt^{-/-}$ cells was not detectable by coimmunoprecipitation assays (data not shown), suggesting that interaction of TRα with CRT *in situ* is transient and that only a small fraction of TRα forms export complexes at any given time. This is consistent with the primarily nuclear population of TR at steady state.

DISCUSSION

Here, we present findings that provide evidence for a previously uncharacterized mechanism for the dynamic shuttling of TRα. We have used a combination of *in vivo* FRAP experiments, *in vitro* digitonin-permeabilized cell nuclear export assays of transiently transfected cells, and GST pull-down assays to investigate aspects of TRα subcellular trafficking. Taken together, our data suggest a novel export mechanism in which CRT directly binds TRα, and CRT and CRM1 work cooperatively to promote rapid, efficient export of TRα from the nucleus (Fig. 9). Alternatively, when the CRM1 pathway is blocked or CRT levels are increased under cellular stress, CRT can act independently as a less efficient exportin. $crt^{-/-}$ cell lines fail to support nuclear export of TRα, suggesting that CRT is indispensable for TRα nuclear export. Thus, CRT may be the most important component of the TRα nuclear export pathway. These data suggest that CRT deficiency prevents CRM1 interacting either directly or indirectly with TRα, and inhibits both cooperative and autonomous TRα export as a consequence.

Prior to this study, the role that CRT plays in nuclear export was a subject of debate. Previously, CRT was thought to reside

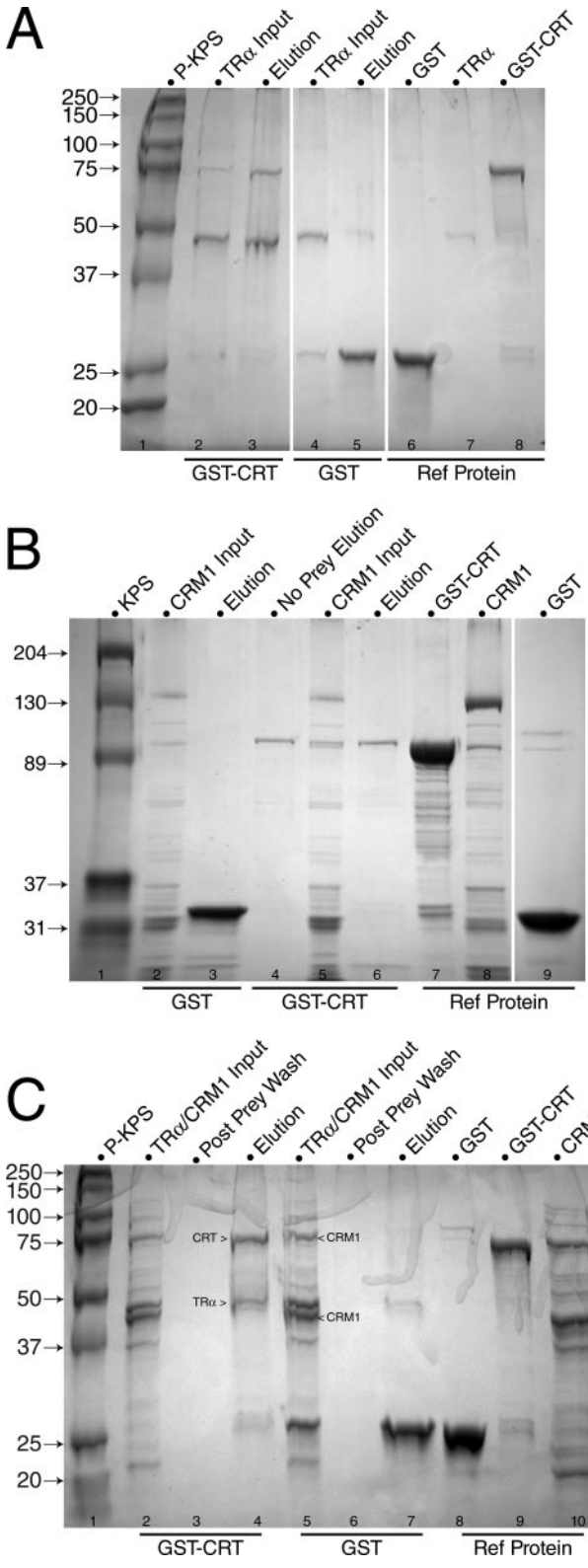

FIGURE 8. **Thyroid hormone receptor (TRα) interacts directly with CRT.** *In vitro* binding interactions were examined by GST pull-down assays. *A*, His-TRα (46 kDa) was retained by GST-CRT bait (*lane 3*, elution), whereas the negative control GST-only bait did not retain TRα (*lane 5*, elution). *Lane 1*, Bio-Rad prestained Kaleidoscope protein molecular mass standards, given in kDa (P-KPS); *lanes 2* and *4*, TRα protein inputs; *lanes 6–8*, reference protein samples. *B*, CRM1 alone was not retained on either GST-CRT (*lane 3*, elution) or negative control GST-only bait (*lane 6*, elution). *Lane 1*, Bio-Rad Kaleidoscope protein molecular mass standards, given in kDa (KPS); *lanes 2* and *5*, His-CRM1 flow-through (*input*); *lane 4*, no prey input, GST-CRT bait elution; *lanes 7–9*, reference protein samples. *C*, TRα binds CRT, but His-CRM1 does not interact directly with the TRα-CRT complex. His-TRα was retained by GST-CRT bait from the combined TRα:His-CRM1 input, whereas the His-CRM1 was not retained (*lane 4*, elution). The negative control GST-only bait did not retain either TRα or His-CRM1 (*lane 7*, elution). *Lane 1*, Bio-Rad prestained Kaleidoscope protein molecular mass standards, given in kDa (P-KPS); *lanes 2* and *5*, His-tagged TRα and CRM1 input; *lanes 3* and *6*, post-prey binding wash samples; *lanes 8–10*, reference protein samples. The His-CRM1 input included full-length CRM1 and lower molecular weight degradation products, as indicated.

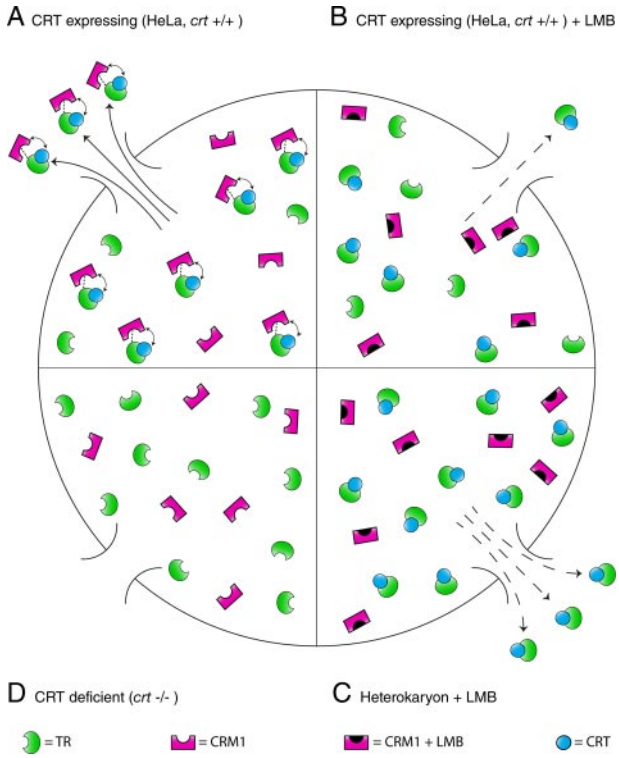

FIGURE 9. **Model for nuclear export of thyroid hormone receptor (TRα) involving a cooperative CRT and CRM1-mediated pathway.** *A,* nuclear export complex in cells expressing CRT (HeLa, $crt^{+/+}$) in which CRT binding promotes a cooperative export pathway involving CRM1. This cooperative interaction is indicated by the *double-headed curved arrow*. CRM1 binding to TRα may require additional factors (indicated by *dashed line*). Although CRT levels are low under these conditions, export of TRα is efficient and rapid export is observed. *B,* inefficient nuclear export of TRα in cells expressing CRT (HeLa, $crt^{+/+}$) occurs upon treatment with LMB. CRM1 is inactivated but CRT can still support modest export autonomously. *C,* rapid export of TRα occurs even in the presence of LMB upon PEG-induced heterokaryon fusion. Although the CRM1 pathway is inactivated, transient CRT release from the ER renders sufficient CRT levels to support rapid export of TRα. *D,* $crt^{-/-}$ cells do not support nuclear export of TRα because CRT is not present to facilitate the CRM1-dependent component of the export pathway.

permanently within the ER lumen where it participates in the maturation of newly synthesized proteins and sequesters Ca^{2+}. In addition to its prominence in the ER, however, increasing numbers of reports have suggested that CRT may in fact be present in small fractions in other cellular compartments. For example, CRT appears to interact with a ubiquitin-like nuclear protein in the nucleus of rice cells (34). Moreover, CRT also localizes to the nuclear matrix of some carcinoma cells and assists in chromatin formation (35). All of these data suggest that CRT is likely to possess an evolutionarily conserved ability to access the nucleus, where it appears to serve multiple functions. Recently, a mechanism involving the post-translational

processing and retrotranslocation of CRT from the ER to the cytoplasm has been identified, suggesting a potential pathway for CRT to subsequently gain access to the nucleus via import (41).

Although low levels of CRT are found in multiple cellular compartments, the majority of CRT present in heterokaryons immediately after cell fusion comes as a result of ER disruption and its release from the ER lumen (29). Although TRα export was inhibited in $crt^{-/-}$ monokaryons, rapid shuttling and fluorescence equilibration was observed between nuclei of heterokaryons. For CRT to mediate export of TRα from $crt^{-/-}$ nuclei, presumably it must first be imported into these same nuclei. Following import, CRT could then interact with TRα and facilitate its nuclear export. Our *in vitro* nuclear export assays suggest that whereas CRT is necessary for efficient export, there is also an additional factor (or factors) in the cytosol required for its nuclear import, its role in the export of TRα, or both. Based on our *in vivo* FRAP experiments, our *in vitro* nuclear export assays, and our Western blot analysis of RRL composition, we suggest that at least one of these additional factors is the exportin CRM1.

In both HeLa and $crt^{+/+}$ cell lines, TRα displayed rapid nucleocytoplasmic shuttling in the absence of LMB. Although the precise mechanism by which this export occurs remains to be determined, there are several potential explanations. CRT and CRM1 could undergo a conformational shift that maximizes interaction with components of the nuclear pore complex, thus expediting the export process. Alternatively, CRM1 could increase the affinity of CRT for TRα allowing for more efficient export. In any case, the fluorescence equilibration between photobleached and unbleached nuclei in monokaryons of either cell type (HeLa $t_{½} = 40$ min, $crt^{+/+}$ $t_{½} = 10$ min) indicates that TRα shuttles rapidly under these conditions.

As treatment with LMB results in covalent modification of a critical cysteine residue within CRM1 (42), this potential cooperative interaction with CRT may be abolished upon LMB treatment. As such, CRT may still be capable of binding TRα and facilitating export, albeit to a lesser extent. This would explain our results in which TRα shuttling in HeLa and $crt^{+/+}$ monokaryons occurs only slowly after treatment with LMB.

Finally, our model takes into account the cell fusion-dependent release of CRT during heterokaryon experiments (29) and explains the stark contrast between LMB-insensitive TRα shuttling in heterokaryons (1) *versus* LMB-sensitive shuttling in monokaryons (present study). Although CRT may be the limiting factor in TRα nuclear export under normal circumstances, this limitation is countered by the increased efficiency of export resulting from the cooperative pathway involving CRM1 (Fig. 9). Although CRM1 is undoubtedly inactivated by LMB treatment in heterokaryons, the attenuated nucleocytoplasmic shuttling expected may not be observed due to the increased cytosolic levels of CRT resulting from PEG-induced cell fusion. Under these conditions, the relatively low levels of CRT found within the nucleus or cytosol under normal circumstances would be markedly increased and its low levels would no longer be limiting. Although, according to this model, autonomous CRT-mediated export of TRα is not as efficient as cooperative export in the presence of CRM1, the sheer increase in free CRT directly after cell fusion may be enough to overcome this deficiency and allow rapid nuclear export to proceed in the presence of LMB (Fig. 9).

Previously, the only support for the hypothesis that CRT mediates export of TR was the finding that the DBD of TRβ is sufficient to confer nuclear export when fused to a GFP reporter. The DBDs of TRβ and GR share 43% sequence homology and, most importantly, the amino acids predicted to be key for CRT binding are conserved (12). Thus, it is not unreasonable to propose that the TRβ DBD could also interact directly with CRT, as has been shown for the GR DBD (8). Examining the specific nucleocytoplasmic shuttling properties of TRα domains within CRT-deficient and CRT-expressing cell lines will provide valuable insight into the physical basis for TRα binding of CRT. Comprehensive analysis of the effects of mutations by *in vitro* binding assays and *in vivo* functional assays should help to identify and clarify those specific amino acid sequences required for nuclear export, as well as nuclear import, of TRα.

In a prior study we showed that *in vitro*-generated ^{35}S-labeled TRα does not interact with purified CRM1 in a His pull-down assay (28). However, most CRM1-dependent NESs bind CRM1 with low affinity and often require additional adapter proteins to serve as a bridge between CRM1 and the cargo protein being exported (3, 43). For example, Ran-binding protein 3 (RanBP3) directly binds CRM1 in the nucleus and increases the affinity of CRM1 for NES containing cargo as well as RanGTP (44, 45). In addition, RanBP3 binding also maximizes the interaction of the CRM1 export complex with nucleoporins of the nuclear pore complex (44). Similar conditions are observed for CRM1 binding of other regulatory proteins that participate in nucleocytoplasmic shuttling. Although steroid receptor coactivator-1 contains two clusters of hydrophobic amino acids similar to the classic leucine-rich NES associated with CRM1-mediated nuclear export, this protein failed to accumulate within the nuclei of COS-7 cells when these regions were mutated even though its export was sensitive to LMB (46). Presumably then, an unknown adapter protein that is recognized by both CRM1 and steroid receptor coactivator-1 accounts for the nuclear accumulation of steroid receptor coactivator-1 upon LMB treatment. Other examples include both the 60 S and 40 S ribosomal subunits of the yeast *Saccharomyces cerevisiae.* These large complexes undergo CRM1-mediated nuclear export in an adapter-dependent manner (47–49). Such situations are analogous to our TRα export pathway model in which additional export factors may be required to facilitate the CRM1-dependent component of TRα translocation from the nucleus to cytoplasm.

The model presented here explains several previously anomalous observations relating to CRT, CRM1, and nuclear receptor export in general. There is certainly a discrepancy between the shuttling kinetics of nuclear receptors in a heterokaryon system *versus* under other experimental conditions, such as those reported in Walther *et al.* (29). Particularly striking is the disparity observed between protein shuttling within *in vivo* monokaryon experiments compared with the interspecies heterokaryon assay. Here, for the first time, the observation that some nuclear receptors such as TRα (present study) and GR

(50, 51) rely in part on CRM1-dependent nuclear export can be reconciled with the observation that cell lines deficient in CRT expression, but retaining their CRM1 activity, fail to support nuclear export of the same proteins (8) (present study).

Interestingly, we have also shown that the p53 tumor suppressor protein displays highly reduced shuttling kinetics in $crt^{+/+}$ monokaryons as compared with heterokaryon assays using HeLa and NIH/3T3 cells.[5] Although the significance of these observations remain to be determined, they again highlight the complexity of nucleocytoplasmic transport pathways and point to a similar discrepancy between p53 shuttling under *in vitro* and *in vivo* conditions. As p53 undergoes nuclear export in a CRM1-dependent manner (52–55), this observation should be considered when designing experiments that attempt to utilize p53 as a control for CRM1 activity.

These data provide insight into the nuclear export pathway of TRα and suggest a possible mechanism by which other shuttling proteins may use complex and, to some extent, functionally redundant export modes involving both characterized pathways (CRM1) and a multitude of other chaperones. In addition, these results also represent a novel role in nuclear export for the functionally diverse protein CRT. Although more research will be necessary to precisely determine the significance of this cooperative export pathway, regulation of TRα target genes may be influenced in several ways. Inefficient TRα nuclear export in the absence of CRT could, for example, be indicative of an evolved compensatory mechanism to up-regulate the transcription of genes involved in similar cellular processes as the numerous ones that have been identified for CRT. Conversely, rapid shuttling of TRα dependent on an intact cooperative export pathway may be representative of a general mechanism to clear shuttling transcription factors from the nucleus under physiological conditions. This cooperative CRM1/CRT-mediated nuclear export pathway may be relevant to related members of the nuclear receptor superfamily other than TRα. Identification of this export pathway and other mechanisms by which nuclear receptors exit the nucleus will contribute substantially to understanding the regulatory activity of these proteins. One challenge for the future will be to examine how regulation of this cellular compartmentalization is impaired or altered in the case of aberrant nuclear receptor expression. In addition, defining how nuclear export integrates TRα activity with other signaling pathways may provide important clues as to the mode of action of mutant TRs that are responsible for a host of pathological conditions including cancer (56–58).

REFERENCES

1. Bunn, C. F., Neidig, J. A., Freidinger, K. E., Stankiewicz, T. A., Weaver, B. S., McGrew, J., and Allison, L. A. (2001) *Mol. Endocrinol.* **15,** 512–533
2. Bonamy, G. M., and Allison, L. A. (2006) *Nucl. Recept. Signal.* **4,** e008
3. Cook, A., Bono, F., Jinek, M., and Conti, E. (2007) *Annu. Rev. Biochem.* **76,** 647–671
4. Pemberton, L. F., and Paschal, B. M. (2005) *Traffic* **6,** 187–198
5. la Cour, T., Kiemer, L., Molgaard, A., Gupta, R., Skriver, K., and Brunak, S. (2004) *Protein Eng. Des. Sel.* **17,** 527–536
6. la Cour, T., Gupta, R., Rapacki, K., Skriver, K., Poulsen, F. M., and Brunak, S. (2003) *Nucleic Acids Res.* **31,** 393–396
7. Shank, L. C., and Paschal, B. M. (2005) *Crit. Rev. Eukaryotic Gene Expression* **15,** 49–73
8. Black, B. E., Holaska, J. M., Rastinejad, F., and Paschal, B. M. (2001) *Curr. Biol.* **11,** 1749–1758
9. Burns, K., Duggan, B., Atkinson, E. A., Famulski, K. S., Nemer, M., Bleackley, R. C., and Michalak, M. (1994) *Nature* **367,** 476–480
10. Dedhar, S., Rennie, P. S., Shago, M., Hagesteijn, C. Y., Yang, H., Filmus, J., Hawley, R. G., Bruchovsky, N., Cheng, H., Matusik, R. J., and Giguère, V. (1994) *Nature* **367,** 480–483
11. Holaska, J. M., and Paschal, B. M. (1998) *Proc. Natl. Acad. Sci. U. S. A.* **95,** 14739–14744
12. Dedhar, S., Rennie, P. S., Shago, M., Hagesteijn, C. Y. L., Yang, H., Filmus, J., Hawley, R. C., Bruchorsky, N., Cheng, H., Matusik, R.J., and Giguere, V. Holaska, J. M., Black, B. E., Love, D. C., Hanover, J. A., Leszyk, J., and Paschal, B. M. (2001) *J. Cell Biol.* **152,** 127–140
13. Mery, L., Mesaeli, N., Michalak, M., Opas, M., Lew, D. P., and Krause, K. H. (1996) *J. Biol. Chem.* **271,** 9332–9339
14. Krause, K. H., and Michalak, M. (1997) *Cell* **88,** 439–443
15. Holaska, J. M., Black, B. E., Rastinejad, F., and Paschal, B. M. (2002) *Mol. Cell. Biol.* **22,** 6286–6297
16. Li, S. S., Forslow, A., and Sundqvist, K. G. (2005) *J. Immunol.* **174,** 654–661
17. Coppolino, M. G., Woodside, M. J., Demaurex, N., Grinstein, S., St-Arnaud, R., and Dedhar, S. (1997) *Nature* **386,** 843–847
18. Leung-Hagesteijn, C. Y., Milankov, K., Michalak, M., Wilkins, J., and Dedhar, S. (1994) *J. Cell Sci.* **107,** 589–600
19. Bohlson, S. S., Fraser, D. A., and Tenner, A. J. (2007) *Mol. Immunol.* **44,** 33–43
20. Donnelly, S., Roake, W., Brown, S., Young, P., Naik, H., Wordsworth, P., Isenberg, D. A., Reid, K. B., and Eggleton, P. (2006) *Arthritis Rheum.* **54,** 1543–1556
21. Hattori, K., Nakamura, K., Hisatomi, Y., Matsumoto, S., Suzuki, M., Harvey, R. P., Kurihara, H., Hattori, S., Yamamoto, T., Michalak, M., and Endo, F. (2007) *Mol. Genet. Metab.* **91,** 285–293
22. Lozyk, M. D., Papp, S., Zhang, X., Nakamura, K., Michalak, M., and Opas, M. (2006) *BMC Dev. Biol.* **6,** 54
23. Mesaeli, N., Nakamura, K., Zvaritch, E., Dickie, P., Dziak, E., Krause, K. H., Opas, M., MacLennan, D. H., and Michalak, M. (1999) *J. Cell Biol.* **144,** 857–868
24. Chandran, U. R., and DeFranco, D. B. (1992) *Mol. Endocrinol.* **6,** 837–844
25. Madan, A. P., and DeFranco, D. B. (1993) *Proc. Natl. Acad. Sci. U. S. A.* **90,** 3588–3592
26. Maruvada, P., Baumann, C. T., Hager, G. L., and Yen, P. M. (2003) *J. Biol. Chem.* **278,** 12425–12432
27. Hache, R. J., Tse, R., Reich, T., Savory, J. G., and Lefebvre, Y. A. (1999) *J. Biol. Chem.* **274,** 1432–1439
28. DeLong, L. J., Bonamy, G. M., Fink, E. N., and Allison, L. A. (2004) *J. Biol. Chem.* **279,** 15356–15367
29. Walther, R. F., Lamprecht, C., Ridsdale, A., Groulx, I., Lee, S., Lefebvre, Y. A., and Haché, R. J. (2003) *J. Biol. Chem.* **278,** 37858–37864
30. Guo, L., Nakamura, K., Lynch, J., Opas, M., Olson, E. N., Agellon, L. B., and Michalak, M. (2002) *J. Biol. Chem.* **277,** 50776–50779
31. Prufer, K., and Barsony, J. (2002) *Mol. Endocrinol.* **16,** 1738–1751
32. Mesaeli, N., and Phillipson, C. (2004) *Mol. Biol. Cell* **15,** 1862–1870
33. Jethmalani, S. M., Henle, K. J., Gazitt, Y., Walker, P. D., and Wang, S. Y. (1997) *J. Cell Biochem.* **66,** 98–111
34. Sharma, A., Isogai, M., Yamamoto, T., Sakaguchi, K., Hashimoto, J., and Komatsu, S. (2004) *Plant Cell Physiol.* **45,** 684–692
35. Kobayashi, S., Uchiyama, S., Sone, T., Noda, M., Lin, L., Mizuno, H., Matsunaga, S., and Fukui, K. (2006) *Cytogenet. Genome Res.* **115,** 10–15
36. Adam, S. A., Marr, R. S., and Gerace, L. (1990) *J. Cell Biol.* **111,** 807–816
37. Weis, K. (2003) *Cell* **112,** 441–451
38. Fried, H., and Kutay, U. (2003) *Cell Mol. Life Sci.* **60,** 1659–1688
39. Corbett, E. F., Michalak, K. M., Oikawa, K., Johnson, S., Campbell, I. D., Eggleton, P., Kay, C., and Michalak, M. (2000) *J. Biol. Chem.* **275,** 27177–27185
40. Andrin, C., Pinkoski, M. J., Burns, K., Atkinson, E. A., Krahenbuhl, O.,

[5] M. E. Grespin and L. A. Allison, unpublished results.

Hudig, D., Fraser, S. A., Winkler, U., Tschopp, J., Opas, M., Bleackley, R. C., and Michalak, M. (1998) *Biochemistry* **37,** 10386–10394
41. Afshar, N., Black, B. E., and Paschal, B. M. (2005) *Mol. Cell. Biol.* **25,** 8844–8853
42. Kudo, N., Matsumori, N., Taoka, H., Fujiwara, D., Schreiner, E. P., Wolff, B., Yoshida, M., and Horinouchi, S. (1999) *Proc. Natl. Acad. Sci. U. S. A.* **96,** 9112–9117
43. Kutay, U., and Guttinger, S. (2005) *Trends Cell Biol.* **15,** 121–124
44. Lindsay, M. E., Holaska, J. M., Welch, K., Paschal, B. M., and Macara, I. G. (2001) *J. Cell Biol.* **153,** 1391–1402
45. Englmeier, L., Fornerod, M., Bischoff, F. R., Petosa, C., Mattaj, I. W., and Kutay, U. (2001) *EMBO Rep.* **2,** 926–932
46. Amazit, L., Alj, Y., Tyagi, R. K., Chauchereau, A., Loosfelt, H., Pichon, C., Pantel, J., Foulon-Guinchard, E., Leclerc, P., Milgrom, E., and Guiochon-Mantel, A. (2003) *J. Biol. Chem.* **278,** 32195–32203
47. West, M., Hedges, J. B., Lo, K. Y., and Johnson, A. W. (2007) *J. Biol. Chem.* **282,** 14028–14037
48. Hedges, J., Chen, Y. I., West, M., Bussiere, C., and Johnson, A. W. (2006) *J. Biol. Chem.* **281,** 36579–36587
49. Seiser, R. M., Sundberg, A. E., Wollam, B. J., Zobel-Thropp, P., Baldwin, K., Spector, M. D., and Lycan, D. E. (2006) *Genetics* **174,** 679–691
50. Savory, J. G., Hsu, B., Laquian, I. R., Giffin, W., Reich, T., Haché, R. J., and Lefebvre, Y. A. (1999) *Mol. Cell. Biol.* **19,** 1025–1037
51. Itoh, M., Adachi, M., Yasui, H., Takekawa, M., Tanaka, H., and Imai, K. (2002) *Mol. Endocrinol.* **16,** 2382–2392
52. Freedman, D. A., and Levine, A. J. (1998) *Mol. Cell. Biol.* **18,** 7288–7293
53. Rittinger, K., Budman, J., Xu, J., Volinia, S., Cantley, L. C., Smerdon, S. J., Gamblin, S. J., and Yaffe, M. B. (1999) *Mol. Cell* **4,** 153–166
54. Lain, S., Xirodimas, D., and Lane, D. P. (1999) *Exp. Cell Res.* **253,** 315–324
55. Stommel, J. M., Marchenko, N. D., Jimenez, G. S., Moll, U. M., Hope, T. J., and Wahl, G. M. (1999) *EMBO J.* **18,** 1660–1672
56. Gonzalez-Sancho, J. M., Garcia, V., Bonilla, F., and Munoz, A. (2003) *Cancer Lett.* **192,** 121–132
57. Cheng, S. Y. (2003) *Mol. Cell. Endocrinol.* **213,** 23–30
58. Bonamy, G. M., Guiochon-Mantel, A., and Allison, L. A. (2005) *Mol. Endocrinol.* **19,** 1213–1230